npj | vaccines

Article

Published in partnership with the Sealy Institute for Vaccine Sciences

https://doi.org/10.1038/s41541-025-01329-0

Novel enzymatic DNA produced from a text file achieves comparable immune responses as plasmid vaccine

James Fuller[1], Erik Kvam[2] ✉, Sandrine Creton[3], Courtney Hall[4], Nicholas J. Tursi[5,6], Kerry Blatney[5], Rebecca Ryan[3], Xavier Godron[3], David B. Weiner[5], Winston Timp[4], Weston Griffin[2], John Nelson[2] & Deborah H. Fuller[1] ✉

DNA vaccines have garnered considerable attention due to their recent success in humans for SARS-CoV-2 and immunotherapy for cancer. However, conventional methods for creating and manufacturing DNA vaccines at-scale are slow and rate-limiting for timely response. Herein, we introduce a rapid and completely synthetic workflow that harnesses enzymes to create bulk DNA from a sequence text file. This synthetic workflow termed Enzymatic DNA Synthesis & Rolling-Circle Amplification (EDS-RCA) leverages multiple enzymes to print DNA oligos and assemble them into genes prior to cloning into circular constructs for rolling-circle amplification (RCA). We show that the resulting EDS-RCA DNA elicits comparable vaccine immunogenicity as standard plasmid format, despite the DNA being a large concatemeric repeat. The EDS-RCA method generated the hemagglutinin gene of H1N1 at a mean per-base error rate as low as ~1 mutation every 10,000 bases and, upon DNA vaccination, elicited strong antibody and cellular immune responses. Skin delivery of EDS-DNA using gene gun facilitated striking vaccine dose-sparing capabilities in comparison to intramuscular electroporation methods. In total, DNA vaccines produced by EDS-RCA are immunogenic and amenable to numerous delivery-modalities with preclinical mouse models and could offer an alternative for rapid scale-up of DNA vaccines for future human use.

Recent success of synthetic mRNA vaccines has ushered in a new era of nucleic acid technology that is revolutionizing vaccine development and offers accelerated design and synthetic production to address a wide range of diseases. Now, further gains in overall process efficiency and flexibility are desired to accelerate the pace of innovation for DNA- and RNA-based vaccines and therapies. For example, faster production of DNA is required to reduce the overall turnaround time from months to days. In addition, agile industrial processes are desired to enable both personalized manufacturing (i.e., single-patient doses for cancer vaccines) and mass production for large populations in short time (i.e., rapid response to an emerging pandemic). New capabilities are also needed to remove fermentative dependencies (i.e. antibiotic resistance and other prokaryotic DNA elements) from humanized sequences encoding nucleic acid vaccines or therapies. To mitigate these needs with greater speed and flexibility, enzymatic DNA production is emerging as a solution by decoupling manufacturing steps from live cells in bioreactors (as the current benchmark for DNA preparation using bacteria)[1–3].

Historically, polymerase chain reaction (PCR) is the gold standard for enzymatic production of synthetic linear expression cassettes, and promising vaccine results have been obtained from PCR-generated linear DNA upon in vivo administration[4–6]. However, PCR-based production of synthetic DNA is not necessarily "cell-free" because bacterial-derived plasmids are often preferred PCR templates. Moreover, key challenges exist for mass production of DNA using PCR, specifically (i) volumetric scale-up (due to physical limitations of precisely heating and cooling large reaction volumes), and (ii) systematic DNA replication errors (i.e., "jackpot" mutations), which are risked with each thermocycling round because the DNA produced by each round is directly templated for further DNA polymerization. Moreover, when administered directly as a DNA vaccine, PCR-generated DNA

[1]Department of Microbiology, University of Washington, Seattle, WA, USA. [2]GE HealthCare Technology & Innovation Center, One Research Circle, Niskayuna, NY, USA. [3]DNA Script Inc., Le Kremlin-Bicêtre, France. [4]Department of Biomedical Engineering, Johns Hopkins University, Baltimore, MD, USA. [5]Vaccine and Immunotherapy Center, The Wistar Institute, Philadelphia, PA, USA. [6]Perelman School of Medicine, University of Pennsylvania, Philadelphia, PA, USA. ✉e-mail: kvame@gehealthcare.com; fullerdh@uw.edu

requires chemical modification to prevent degradation of exposed linear ends, otherwise effective DNA stability is decreased in vivo[4,6].

To circumvent the practical challenges posed by PCR, *E. coli*-produced plasmid DNA can be enzymatically processed into linear expression cassettes or subsequently ligated into covalently closed DNA (MIDGE® vectors) to achieve promising vaccine outcomes[7]. However, because these methods are still fundamentally cell-based, they are subject to potentially long preparative lead times for bacterial fermentation, as well as downstream removal of bacterial-associated impurities (such as endotoxin) from the semi-synthetic DNA product. These challenges are similarly shared by RNA vaccines that rely on enzymatically digested plasmids as raw material input for mRNA production.

To eliminate all dependencies for cell-based plasmids, cell-free DNA assembly processes have been developed using chemically-synthesized oligos to create linear DNA for enzymatic amplification and vaccine preparation[8]. This plasmid-free process involves stitching together synthetic oligonucleotides by assembly-PCR (or overlap extension PCR) and generates linear expression cassettes de novo[9]. Similar approaches have been developed using ligases to assemble synthetic oligonucleotides into linear DNA for faster cloning toward pandemic response[10,11]. However, these synthetic methods depend on chemically-synthesized DNA parts (e.g., phosphoramidite oligo pools, PAGE-purified long oligonucleotides, or double-stranded gBlocks®, for example), which produce substantial hazardous waste streams[12]. Furthermore, practical challenges for bulk-scaling linear DNA by PCR still apply, so a translational gap remains for at-scale vaccine manufacturing from chemically-synthesized oligos. This is especially true of nucleic acid vaccines having large and complex untranslated regions for transcription (e.g., eukaryotic promoters and terminators including polyA tails) because they are difficult to amplify using PCR.

Recently, enzymatic DNA production by rolling-circle amplification (RCA) has emerged as a PCR-free method for scaling up synthetic DNA. Compared to PCR, RCA offers several advantages toward satisfying DNA manufacturing and capacity desires, including (i) scalable implementation as a consequence of being an isothermal reaction, and (ii) no replication-based "jackpot" errors because amplicons extend from the original DNA input molecule via a strand-displacing DNA polymerase[13,14]. Much like roll-to-roll manufacturing, RCA produces a concatenated expression template with numerous copies of the same DNA sequence. To date, all applications of RCA for DNA vaccines have included laborious enzymatic processing of the RCA concatemer into smaller linear expression cassettes (e.g., synDNA™)[15,16] or into closed-end linear DNA (e.g., doggyboneDNA® or dbDNA®)[17,18] based on the premise that small expression cassettes are more easily translocated into host cell nuclei than larger-sized DNA (akin to genomic DNA and artificial chromosomes). Consequently, the general expectation is that unprocessed RCA DNA concatemers would be too large and too complex for effective in vivo use.

Here, we describe a multi-enzymatic approach for obtaining bulk synthetic DNA for immunization that requires no chemical synthesis of DNA parts to complete cell-free mass production. Starting from an in silico DNA sequence, multiple enzymes are leveraged in discrete steps to (i) synthesize DNA oligos, (ii) assemble DNA fragments into full-length genes, (iii) ligate genes into circular vectors, and (iv) scale up DNA by rolling-circle amplification. We report that the resulting EDS-RCA concatemers (which are not further processed into DNA monomers) elicit comparable vaccine outcomes as conventional plasmid. We applied this synthetic approach to produce the hemagglutinin gene of H1N1 at a mean per-base error rate as low as ~1 mutation every 10,000 bases, and upon vaccinating mice, EDS-RCA products achieved strong antibody and cellular immune responses (on par with conventional plasmid DNA) using either biolistic- or electroporation- based delivery methods.

Results

Enzymatic DNA production starting from a text file

Figure 1 illustrates our enzymatic DNA synthesis & rolling-circle amplification (EDS-RCA) workflow, which is completely mediated by enzymes. The HA gene from H1N1 swine flu was selected as a model antigen to demonstrate DNA creation and scale-up by EDS-RCA. Starting from the HA amino acid sequence deposited as GenBank ACP41935.1 (representing May and June serotypes of 2009 California influenza), the DNA coding sequence was in silico optimized (using proprietary DNA Script algorithms for TdT-based enzymatic DNA synthesis) to create an EDS-optimized text file. Before printing this sequence and launching full EDS-RCA production, we investigated if different HA codon usages might influence immunogenicity. To test this hypothesis, we chemically synthesized both the native HA gene sequence and the EDS-optimized text file sequence and cloned these into expression plasmid (pCAGG-MCS-WPRE) under CAGG promoter control. These HA plasmids were then compared in a pilot mouse study using biolistic gene gun (GG) delivery to administer each DNA vaccine into the epidermis. Antibody responses induced by these plasmids were compared to a control vector encoding the traditional mouse codon-optimized HA (under different CMV promoter control). The corresponding results provided in Supplementary Fig. S1 demonstrate that each of the tested HA codon usages (and corresponding promoter contexts) induced comparable antibody responses after prime and boost immunization of the plasmid vaccine. These HA constructs also elicited similar neutralizing antibody responses as measured by hemagglutination inhibition assay (HAI titer, Fig. S1). Taken together, these results demonstrated that the EDS-optimized text file sequence (GenBank PV750927) was suitable for further vaccine development.

We next performed digital-to-physical DNA production by loading the EDS-optimized text file onto a commercial SYNTAX machine to enzymatically print and then purify oligonucleotides into 96-well plates. The total run time was ~16 h and produced 142 oligos (one per well) with a final yield of 300 pmol per well. Sequencing these oligonucleotides revealed a mean average error rate per position of ~0.219% (or approximately 1 error every 456 bases, see Fig. 2A and Supplementary Fig. S3), including deletions and insertions that are more likely to disrupt protein translation than substitutions (i.e., functional rescue via codon wobble). Importantly, this average oligo error rate (driven in part by deletion rates around 0.1% per base) is within the range reported for standard phosphoramidite-based DNA synthesis[19,20]. To reduce the impact of EDS-based error, we implemented various steps during downstream gene assembly, in a manner analogous to error correction practices for chemically synthesized oligos[21].

SYNTAX-printed oligos were pooled and ligated to generate double-stranded blocks of DNA of up to 500 bp in length and 8 blocks were built to cover the entire HA gene. These blocks were subsequently pooled for assembly and amplification of the full HA gene through a "Step 2" assembly PCR (see Fig. 1, middle panel). Sequencing the input blocks and output full-length HA genes revealed that the mean average error rate per position decreased substantially (Fig. 2A). Enzymatic ligation alone (to create blocks) accounted for much of this error reduction (i.e., from ~0.22% on oligos to ~0.11% for blocks, Fig. 2A and Supplementary Fig. S3). Much of this error reduction is explained by complement-based positive selection that is inherent to ligase activity (i.e., how well sticky ends actually base-pair and ligate, versus mismatches that reduce this likelihood)[22,23].

Lastly, the enzymatically-assembled HA gene pool was cloned into expression vector (pCAGG-MCS-WPRE) to mediate DNA scale-up by rolling-circle amplification (see Fig. 1, bottom panel). A plasmid-based chassis is not strictly required for this cloning step but allowed for benchmarking of EDS-RCA products against the conventional state-of-art (i.e., plasmid scale-up by bacterial fermentation). A mixed clone pool comprising ~200+ individual plasmids (each containing enzymatically prepared HA and thus representing ~200+ individual EDS gene assemblies after pooling) was utilized as template for RCA. All resulting DNA products from RCA reactions were maintained in their native concatemeric (hyperbranched[14]) state with no further enzymatic or physical shearing back into smaller DNA monomers. This concatenated DNA product is the final output of our EDS-RCA workflow and represents at least ~10,000–100,000-fold amplification of the original enzymatically-prepared gene. In this manner, the EDS-RCA

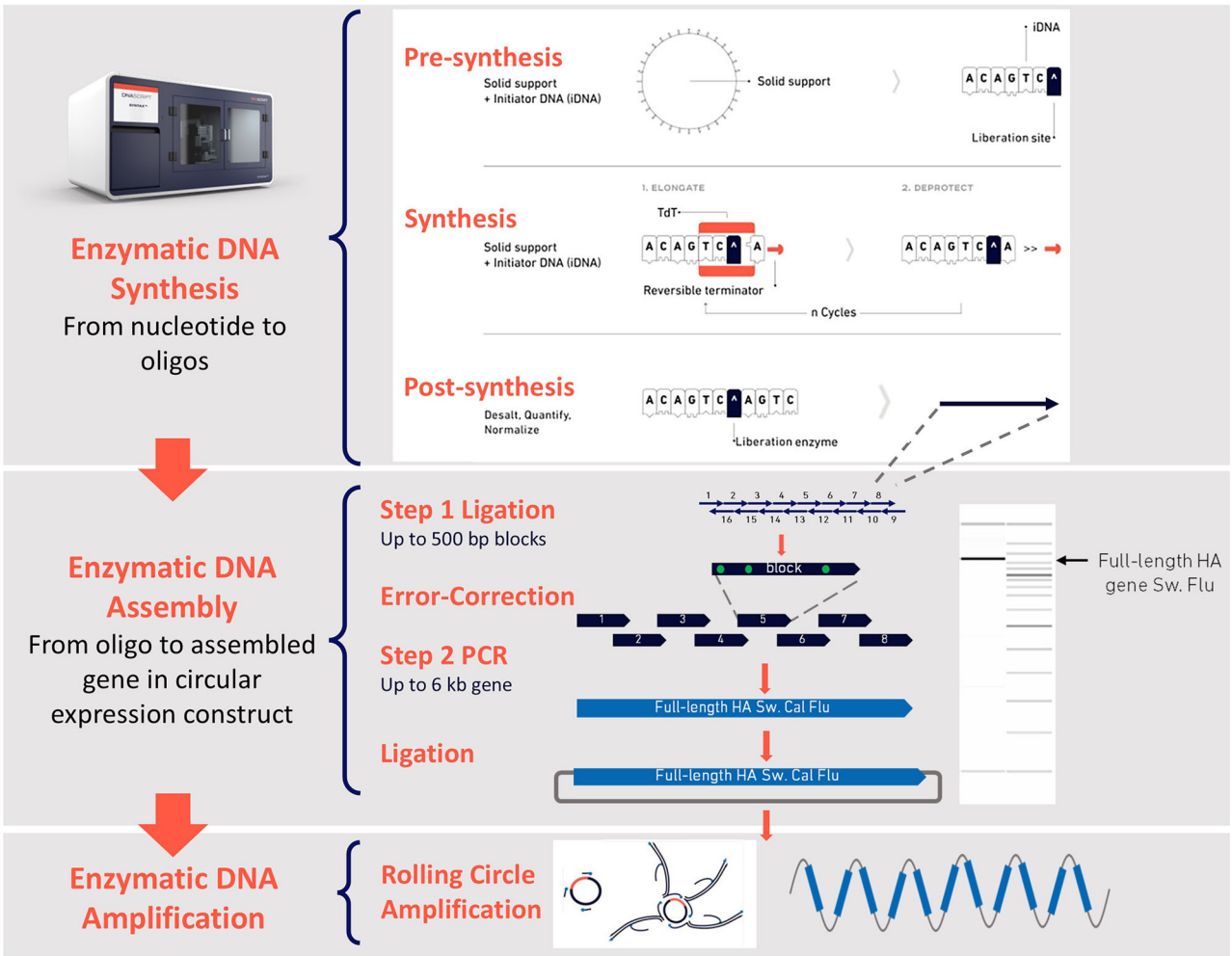

Fig. 1 | Schematic overview of enzymatic DNA synthesis & rolling-circle amplification (EDS-RCA). The top-to-bottom flow shows discrete sub-steps of the integrated EDS-RCA workflow, including enzymatic DNA synthesis, enzymatic DNA assembly, and enzymatic DNA amplification.

workflow facilitates volumetric scale-up of bulk DNA vaccine doses (e.g., from nanograms of template input to milligram/gram-scale RCA outputs).

EDS-RCA DNA induces comparable immunogenicity as plasmid DNA when delivered at all doses via gene gun but not via electroporation

We conducted mouse immunization studies using different plasmid and EDS-RCA constructs to determine initial dosing parameters for biolistic delivery to the skin (GG) or standard intramuscular electroporation (IM-EP). These experiments used early assemblies of enzymatically-prepared HA (~0.086% average error per position, without further error reduction) that were cloned into plasmid (~212 clone pool) and subsequently propagated (non-clonally) by RCA or in bacteria. From this master "pool" we also clonally screened (by Sanger sequencing) and obtained a "perfect" plasmid with no HA mutations, and this Sanger-perfect plasmid was propagated clonally by RCA or in bacteria. Mice were then immunized with plasmid DNA (comprising pooled or perfect HA assemblies) or sequence-matched EDS-RCA DNA (comprising identical pooled or perfect HA assemblies as plasmid chassis) and vaccine doses were delivered across a 10-fold dilution series (2 μg, 0.2 μg, 0.02 μg). Figure 3 shows mouse results after prime and boost vaccine delivery. For all doses tested by biolistic GG, delivery of EDS-RCA DNA induced HA-specific antibody responses at levels comparable to corresponding plasmid chassis (Fig. 3A). Furthermore, there were no significant differences in antibody responses between high and low vaccine doses or between pooled and perfect HA assemblies using the GG delivery method (Fig. 3A). In contrast, using IM-EP delivery, a vaccine dose-dependent antibody response was observed, and for all doses, EDS-RCA DNA induced lower HA antibody responses when compared to plasmid chassis (Fig. 3B). Interestingly, mean HA antibody titers also trended consistently (but insignificantly) lower for pooled HA assemblies delivered by IM-EP compared to perfect HA across identical chassis. We concluded that 0.02 μg DNA doses can induce strong antigenicity via GG delivery of either EDS-RCA product or plasmid chassis, but higher dosing (i.e., at least 0.2 μg for plasmid and 2 μg for EDS-RCA DNA) is required to attain similar antigenicity by standard IM-EP delivery. These results are consistent with literature across multiple animal models wherein delivery of plasmid vaccine by IM-EP or IM has required higher DNA dosing compared to GG to achieve comparable antigenic responses[24–26]. Our results now show that significant dose-sparing of EDS-RCA DNA is achievable using skin delivery versus intramuscular delivery (Fig. 3).

Enzymatic error reduction generates EDS-RCA DNA with higher sequence fidelity

Next, we integrated enzymatic error reduction steps while building the full-length HA gene (Fig. 1, middle panel) to increase final sequence fidelity. Up to three rounds of proprietary enzymatic treatments were implemented on HA blocks and we observed progressively lower average error rates per position, with reproducible performance across technical replicates (Supplementary Fig. S3). PacBio sequencing became essential to quantify error rates after two rounds of enzymatic error reduction because standard Illumina lacks consensus base-calling to eliminate sequencing noise at single DNA-molecule resolution (Supplementary Fig. S3). PacBio sequencing

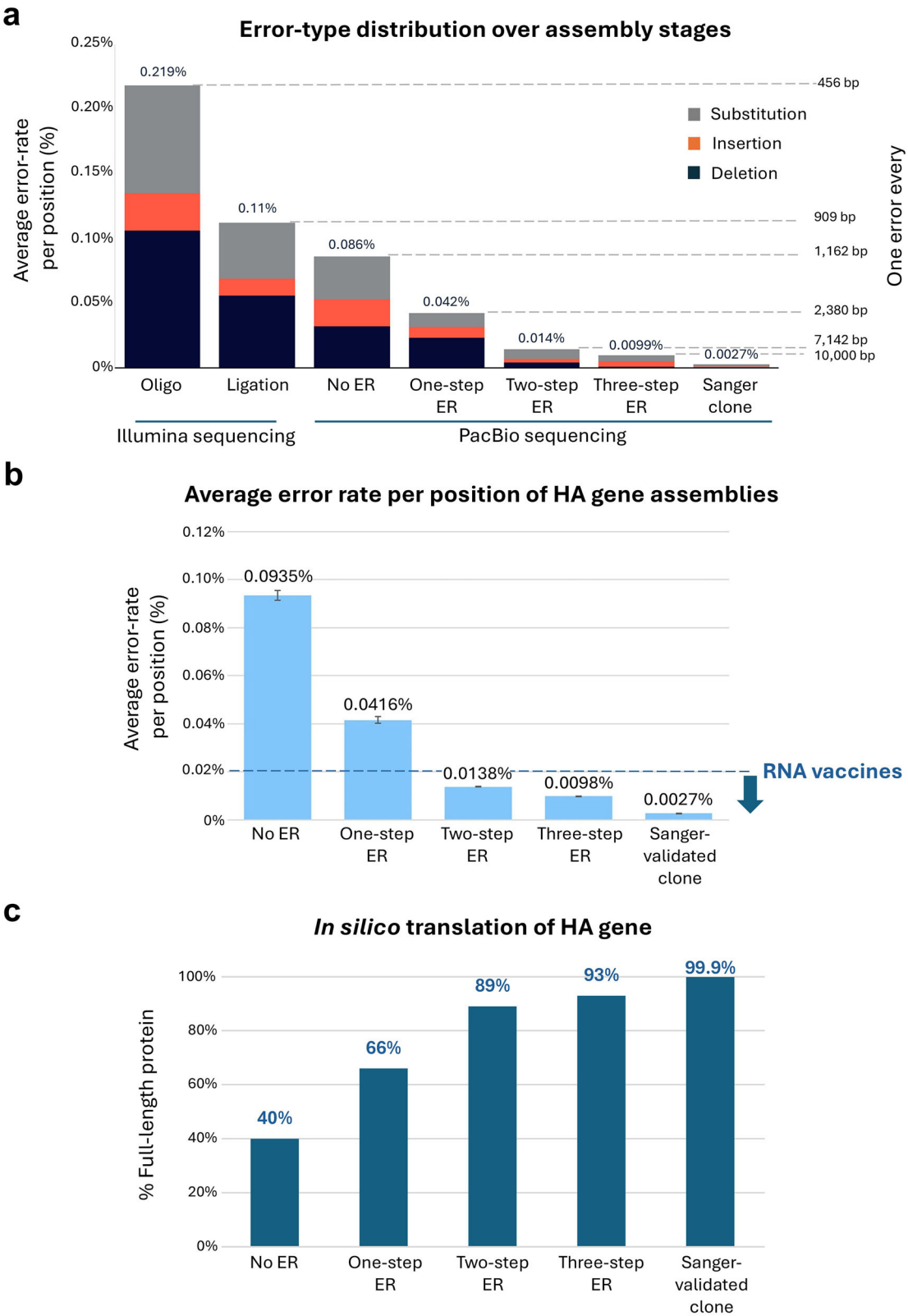

Fig. 2 | Summary of NGS findings over the course of enzymatic gene assembly, including enzymatic error reduction (ER) steps. a Average error rate per synthesized base, as determined by Illumina short-read and PacBio long-read analyses. **b** Average error rate per position of the synthesized HA genes (PacBio sequencing) relative to the threshold reported for general mRNA vaccines (<0.02%). Data from two independent HA assembly rounds are summarized per bar. **c** In silico translation of PacBio reads for quantification of intact (full-length) protein from synthesized HA genes.

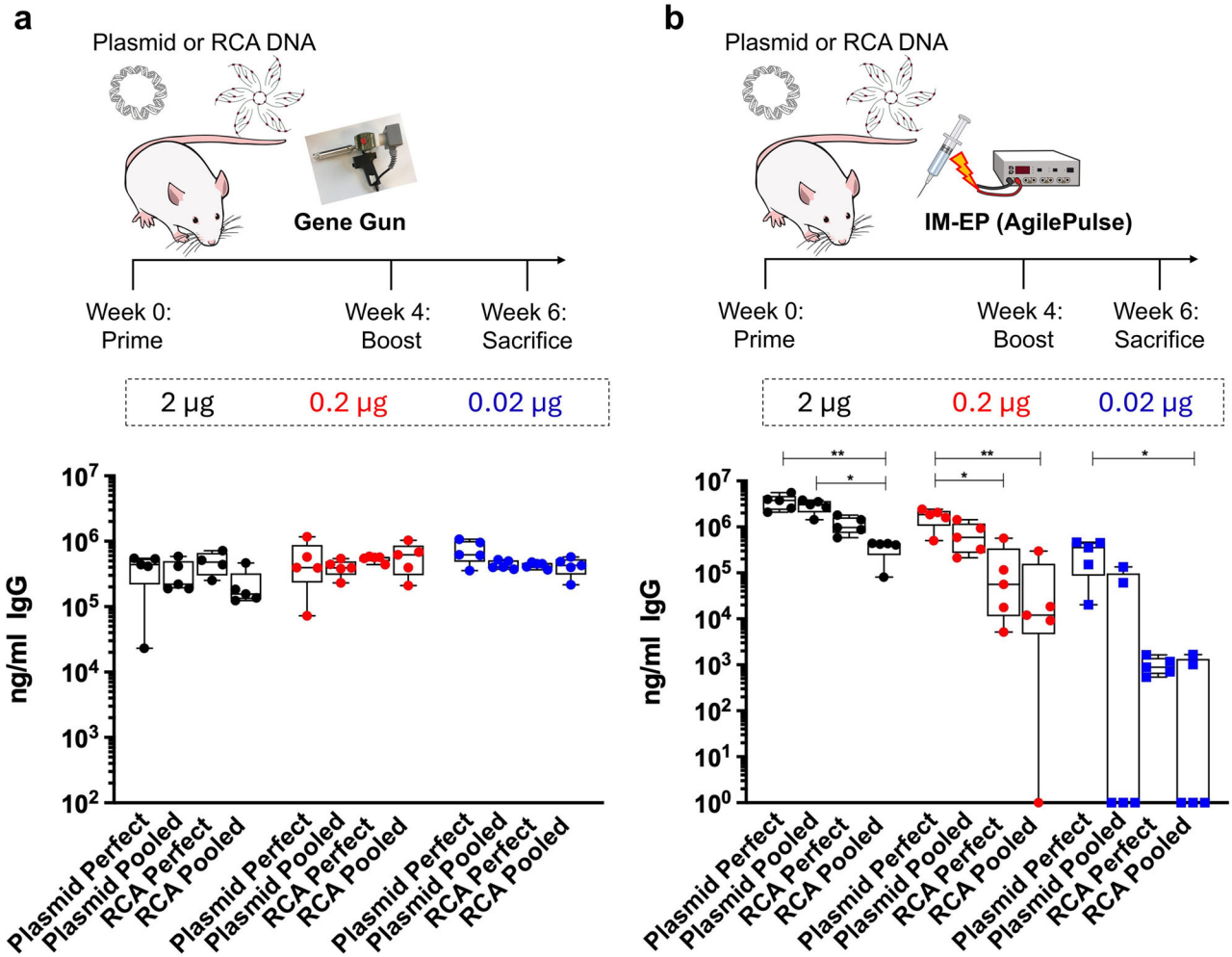

Fig. 3 | Immunogenicity of plasmid and EDS-RCA DNA influenza HA DNA vaccine formulations delivered by gene gun and electroporation. Balb/c mice ($N = 5$ per group) were immunized with a Sanger-perfect assembly of HA or EDS-pooled HA assemblies (without error reduction steps) at week 0 and week 4 and sacrificed at week 6 for quantification of CA09 HA-specific total IgG in serum by ELISA. The indicated vaccine doses of plasmid chassis or EDS-RCA DNA were delivered via epidermal gene gun (**a**) or intramuscular electroporation (IM-EP) (**b**). Doses are color-coded (2 µg in black, 0.2 µg in red, and 0.02 µg in blue). HA-specific antibody responses were measure by ELISA 2 weeks after booster immunization. Each symbol represents an individual mouse. Whisker plots display min to max values for each group, dots represent individual mice. Kruskal-Wallis test with Dunn's multiple comparison was used for comparison between three or more groups. $*p < 0.05$; $**p < 0.01$. Figures were generated using GraphPad Prism version 10.4.2 for MacOS (GraphPad Software, Boston, MA, USA). Certain illustrations are from NIAID NIH BioArt Source (bioart.niaid.nih.gov/bioart/411, bioart.niaid.nih.gov/bioart/283, bioart.niaid.nih.gov/bioart/506, bioart.niaid.nih.gov/bioart/580).

revealed that three rounds of enzymatic treatment generated final HA assemblies at high sequence fidelity (i.e., ~0.0098% average error per base, or less than one error every 10,000 bases, Fig. 2B), which was very close to that of a Sanger-perfect (clonally-isolated) HA (i.e., ~0.0027% average error per base, Fig. 2B). Error reduction steps also reduced the frequency of deletions and insertions such that greater full-length protein was predicted by in silico translation of the PacBio reads (Fig. 2C). Because PacBio sequencing of our Sanger-perfect reference clone involved a PCR step during library prep, we repeated HA sequencing using a "PCR-free" method (which entailed rolling-circle amplification of the Sanger-perfect plasmid followed by digestion of the resulting DNA concatemer with restriction enzymes to obtain linearized HA templates for PacBio sequencing). This PCR-free method similarly returned a mean error rate per position of ~0.003% for the Sanger-perfect plasmid (Fig. 4A). Therefore, even the Sanger-perfect HA reference is not 100% perfect according to next-generation sequencing (NGS), and the trace changes we observed were likely introduced during bacterial-isolation and subculture of this clone. The impact of such trace error is inconsequential since we observed in Fig. 3 that a pooled HA plasmid vaccine comprising >30-fold higher average error still elicited almost equivalent immunogenicity as the clonal Sanger-perfect HA plasmid.

Using analogous "PCR-free" library prep methodology, we next sequenced EDS-RCA DNA products and compared PacBio results to the original HA gene assembly pools (i.e., before cloning into circular expression vector). Digesting EDS-RCA DNA concatemers into DNA monomers provided sufficient depth of coverage for applying maximal read quality filtering (rq = 1). Consequently, PacBio sequencing noise could be efficiently eliminated at single DNA-molecule resolution to better quantify true error rates during EDS-RCA (as evidenced by the Sanger-perfect plasmid at rq =1 in Fig. 4A). We used plasmid-resident restriction enzymes immediately flanking the HA gene to release DNA monomers from EDS-RCA products for downstream PacBio NGS. The product of EDS-RCA after one round of error reduction assembly showed an average error rate similar to the starting HA assembly (0.056% vs 0.04%, respectively, Fig. 4B). After three rounds of enzymatic error reduction, improved HA sequenced fidelity was evident in both the EDS-RCA product and the starting assembly (0.021% vs. 0.01% respectively, Fig. 4C). The slightly higher average error post-RCA likely reflects

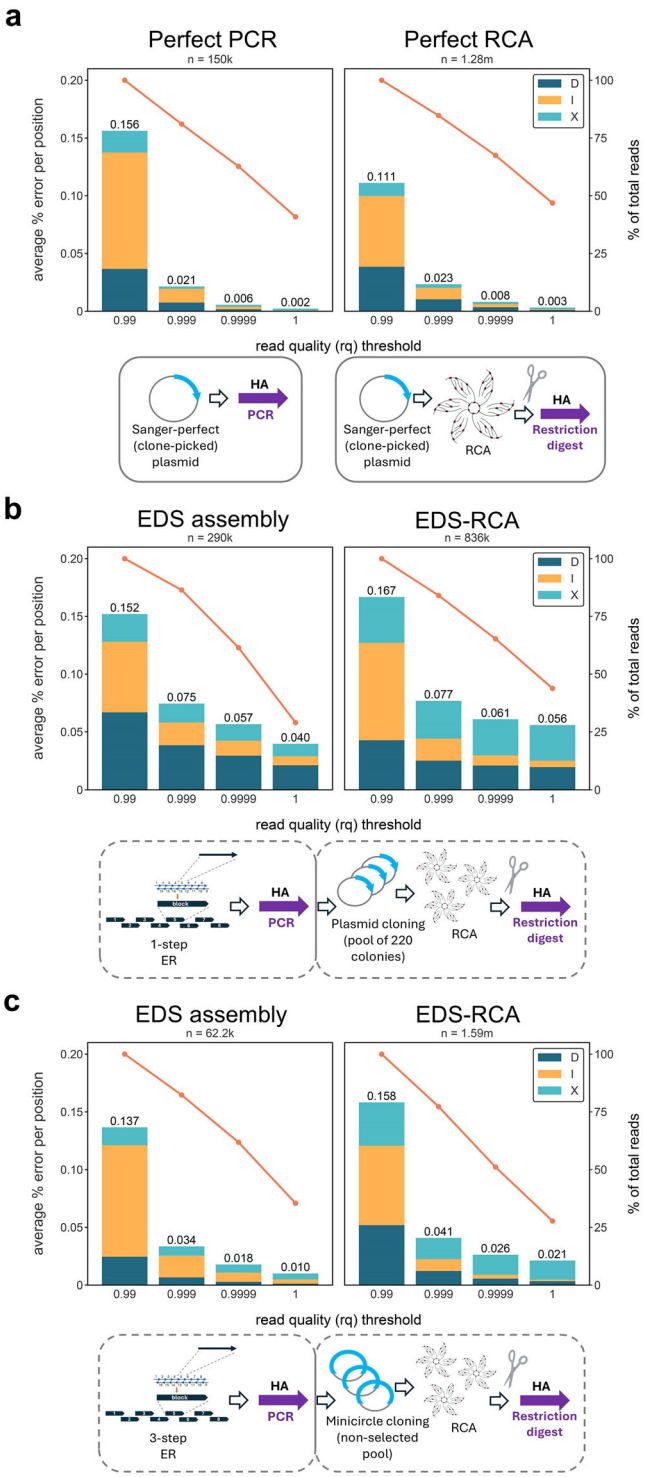

Fig. 4 | Correlation in sequence fidelity before and after EDS-RCA propagation. Average occurrence of deletions (D), insertions (I), and substitutions (X) are color-coded in each bar graph as a function of PacBio read quality (rq) thresholds. Secondary axes depict the percentage of total reads surviving analysis at each rq threshold. Pre-analytical workflow illustrations are provided for clarity and PacBio library prep steps are depicted in purple. **a** Comparison of PCR- versus RCA-propagation of a Sanger-perfect plasmid encoding HA with no mutations (GenBank PV750927). Each bar depicts a different PacBio read quality threshold. **b** Average error per base over the course of EDS-RCA when using a single error-reduction (ER) step during HA synthesis (GenBank PV750927). Each bar depicts a different PacBio read quality threshold. **c** Average error per base over the course of EDS-RCA using a three-step error-reduction (ER) workflow during HA synthesis (GenBank PX367232). Each bar depicts a different PacBio read quality threshold. Scissor illustration is from NIAID NIH BioArt Source (bioart.niaid.nih.gov/bioart/488).

random sampling biases introduced through intermediate cloning since the starting diversity of assembled HA genes were winnowed by ligation into expression vector or vectorette, just prior to the RCA step (see illustrations in Fig. 4). Importantly, the enzyme performing RCA (phi29 DNA polymerase) possesses an extremely low intrinsic error rate, equivalent to ~1 error every 330,000 bases (<0.0003%)[27]. In all, these data demonstrate that modifications to EDS gene assembly can improve the sequence fidelity of the produced EDS-RCA vaccine.

At minimum effective dosing, EDS-RCA DNA delivered by GG and IM-EP induce robust adaptive immune responses

We conducted immunogenicity studies for HA assemblies synthesized with one error reduction step because the resulting average error rate (see Fig. 2B) slightly exceeded the threshold reported for mRNA vaccines under emergency use authorization[28]. It is well known that RNA polymerases are more error-prone than higher fidelity DNA polymerases[29,30], so we set a threshold for acceptable DNA mutations around ~0.02% per position (Fig. 2B) to be consistent to mRNA vaccine precedent. By comparison, errors introduced by amino acid misincorporation during recombinant protein production may occur at even higher rates (i.e., up to 0.1% per translated codon) under certain circumstances[31].

To re-compare immunogenicity between EDS-RCA and plasmid chassis, HA assemblies having ~1 error every 2500 bases (~0.04% per position, Fig. 4B) were cloned into plasmid and subsequently propagated as non-clonal pools by RCA or bacterial culture (~220 mixed positive clones, respectively) in order to sample the diversity of the original HA gene assembly. The corresponding EDS-RCA DNA was maintained in its native concatemeric state and vaccine doses were prepared using two different DNA purification methods: (i) ethanol precipitation (EtOH RCA) or (ii) ion exchange chromatography (IEX RCA). Groups of mice were immunized with these pooled EDS-RCA DNA or plasmid assemblies using to our optimal dosing for GG and IM-EP delivery (i.e., 0.02 μg for GG, and >10-fold higher for plasmid and >100-fold higher for EDS-RCA using IM-EP, see Fig. 3). At these doses, we observed similar magnitudes of HA-specific antibody titers between plasmid chassis and EDS-RCA DNA, regardless of the downstream vaccine purification method employed (i.e., IEX or EtOH) (Fig. 5B). Both GG and IM-EP delivery of EDS-RCA DNA induced comparable IFN-γ T cell responses in spleens (Fig. 5C) and lungs (Fig. 5D) as the plasmid chassis. Consistent with these findings, all tested vaccine formats elicited comparable inhibition of hemagglutination (HAI titer, Fig. 5E) and virus-neutralizing titers against live H1N1 virus in vitro (Fig. 5F). Taken together, these data further demonstrate that the EDS-RCA vaccine induces robust immune responses comparable to plasmid chassis.

We next investigated if the 10-fold higher dosing needed for IM-EP delivery of EDS-RCA (relative to plasmid chassis) was specific to the pulse-waveform used by BTX AgilePulse EP technology. We re-tested identical DNA from Fig. 5, but now using a CELLECTRA-3P device (INOVIO Pharmaceuticals, Inc.) that applies adaptive electroporation and is currently under investigation in human clinical trials[32,33]. We compared the immunogenicity of 0.2 μg and 2.0 μg vaccine doses and selected the IEX preparation of EDS-RCA DNA (since we had observed little difference to EtOH preparation in Fig. 5). Using CELLECTRA-3P, 0.2 μg doses of plasmid chassis induced variable HA-specific IgG antibody responses (similar to EDS-RCA DNA), with some animals failing to seroconvert and, overall, significantly lower antibody responses compared to 2 μg doses (Fig. 6B and Supplementary Fig. S4). Immunization with 2 μg doses showed comparable and robust antibody responses between EDS-RCA DNA and plasmid formats (Fig. 6B and Supplementary Fig. S4). Thus, compared to prior BTX AgilePulse experiments using identical and/or similar DNA (Figs. 5B and 3B, respectively), these CELLECTRA-3P findings suggest that electroporation delivery methods can indeed influence the comparative immunogenicity of DNA vaccines.

We next compared T cell responses after 2 μg immunization by CELLECTRA-3P, using identical DNA from Fig. 5. Both plasmid chassis and EDS-RCA DNA induced robust IFN-γ cell responses as measured by ELISpot (Fig. 6C) and achieved comparably higher responses with CELLECTRA-3P than prior data using BTX AgilePulse (or GG) (Fig. 5C). Flow cytometry analysis of effector T cells revealed that both plasmid chassis and EDS-RCA induced comparable frequencies of IFN-γ and TNF-α secreting $CD8^+$ T cells using CELLECTRA-3P (Fig. 6D, E). Similar trends were also observed for cytokine-secreting effector $CD4^+$ T cells (Fig. 6F–H), albeit plasmid chassis induced statistically higher IFN-γ as well as IL-2 secreting $CD4^+$ T cell numbers than EDS-RCA DNA. In all, these data show that EDS-RCA can efficiently induce robust antibody and T cell responses using adaptive (and clinically-relevant) EP methods in vivo. Interestingly, at equivalent dose-masses, the EDS-RCA DNA and plasmid vaccines trended toward similar immunogenicity profiles using CELLECTRA-3P, much like the prior dose-response relationship established for GG delivery (Figs. 3 and 5). These observations further suggest that comparative study of DNA vaccines is highly influenced by the delivery modality used for immunization.

Minicircle-based EDS-RCA induces similar immune responses as EDS-RCA prepared from plasmid chassis

Having established that EDS-RCA provides a comparable vaccine vehicle to conventional plasmid, we next revised our workflow in Fig. 1 to eliminate plasmid cloning all together. A "plasmid-free" manufacturing process was performed wherein enzymatically-synthesized HA assemblies were ligated into a minicircle "vectorette" chassis lacking prokaryotic DNA elements (i.e., antibiotic resistance and origin of replication that are normally required for clonal selection and bacterial maintenance). Thus, the resulting minicircle vectorette comprises only eukaryotic DNA elements (i.e., CAGG promoter, WPRE enhancer, polyA signal) for expression in mammalian cells. We also implemented triple error-reduction enzymatic workflows that achieved HA DNA molecules with an average error rate per position of ~0.01% (starting gene assembly)—0.021% (following vectorette subcloning and RCA, Fig. 4C), which is consistent with the threshold range established by certain mRNA vaccines[28,29]. It is noteworthy that upon ligating HA assemblies into minicircle vectorette, the resulting ligated circles cannot be clonally selected in bacteria, so RCA is the only means for propagating this minicircle DNA vaccine. Following IEX vaccine purification, the immunogenicity of the minicircle EDS-RCA product was directly compared against plasmid-templated EDS-RCA using the same DNA from Fig. 5 (IEX RCA). Groups of mice were immunized according to our previously determined optimum doses for GG and IM-EP delivery (i.e., 0.02 μg for GG and 2 μg for IM-EP, Fig. 3). Figure 7 shows that both GG and IM-EP delivery resulted in similar magnitudes of HA-specific antibody responses, IFN-γ T cell responses, and HAI titers between the minicircle-based and plasmid-based EDS-RCA products (Fig. 7B–D). Therefore, minicircle vaccine (which cannot be clonally propagated by bacteria and requires RCA) can functionally substitute for plasmid-templated chassis in vivo.

Discussion

We developed a synthetic multi-enzymatic workflow for consecutively creating DNA from a text file and rapidly scaling this DNA (cell-free) for effective in vivo use. We demonstrated herein that an EDS-RCA influenza DNA vaccine—despite being an unprocessed (hyperbranched[14]) DNA concatemer—induced comparable immune responses as a sequence-matched conventional plasmid DNA vaccine. This challenges existing conventional wisdom for large DNA being too complex for effective cell delivery and efficacious in vivo use. Consequently, our results question long-standing practices for laboriously processing DNA from RCA reactions into smaller expression cassettes (e.g., synDNA)[15] or closed linear DNA (e.g., doggyboneDNA)[17,18] prior to use. Indeed, other groups have observed that large and intact RCA DNA transfect tissue culture cells in vitro with comparable expression as plasmid DNA[34–37]. The molecular mechanism for how such large (hyperbranched[14]) RCA DNA mediates effective expression inside cells is still unclear and merits further study.

Our in vivo experiments revealed that vaccine delivery modalities play a significant role in the relative immunogenicity of EDS-RCA DNA vaccines compared to plasmid at the same dose. Specifically, we found that skin delivery by GG elicited robust and concordant HA-specific antibody responses across all tested dose levels, including ultra-low doses (0.02 μg). In contrast, intramuscular delivery via pulse-waveform electroporation (BTX AgilePulse) elicited a dose-dependent antibody response, with plasmid chassis inducing higher antibody titers than the EDS-RCA DNA at all doses. The difference in outcome between these two vaccine delivery modalities is likely due to the ability of GG to achieve more efficient DNA microinjection directly into cells, coupled to the fact that skin, unlike muscle, is rich in

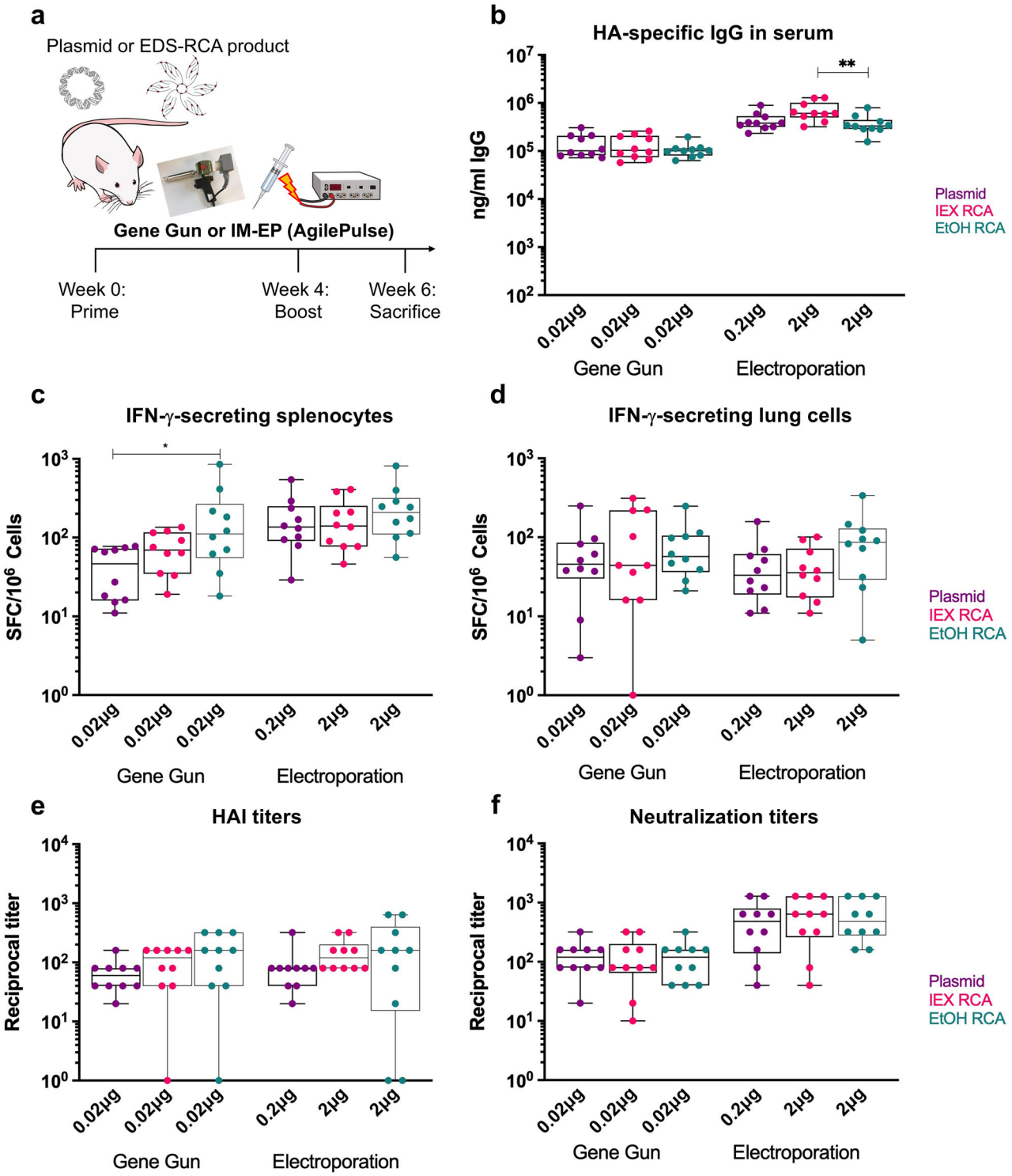

Fig. 5 | Immunogenicity of plasmid and EDS-RCA DNA vaccines delivered at optimum doses via gene gun and electroporation. Balb/c mice ($N = 10$ per group) were immunized via gene gun or electroporation, using the indicated optimum dosing from Fig. 3. EDS-pooled HA assemblies (after a single round of enzymatic error reduction) were delivered by plasmid chassis or as RCA DNA. EDS-RCA DNA vaccine was tested following two different purification methods: ion exchange chromatography (IEX RCA) or ethanol precipitation (EtOH RCA). **a** Schematic of experimental design. Mice were immunized with either pooled plasmid or EDS-RCA DNA at week 0 and week 4 and immune responses were measured 2 weeks after boost (week 6). **b** HA-specific IgG responses in serum measured by ELISA. **c** IFN-γ-secreting T cell responses from spleen measured by ELISpot. **d** IFN-γ-secreting T cell responses from lungs measured by ELISpot. **e** Hemagglutination inhibition (HAI) titers measured against virus. **f** Virus neutralizing assay titers. Whisker plots display min to max values for each group, dots represent individual mice. Kruskal–Wallis test with Dunn's multiple comparison was used for comparison between three or more groups. *$p < 0.05$; **$p < 0.01$. Figures were generated using GraphPad Prism version 10.4.2 for MacOS (GraphPad Software, Boston, MA, USA). Certain illustrations are from NIAID NIH BioArt Source (bioart.niaid.nih.gov/bioart/411, bioart.niaid.nih.gov/bioart/283, bioart.niaid.nih.gov/bioart/506, bioart.niaid.nih.gov/bioart/580).

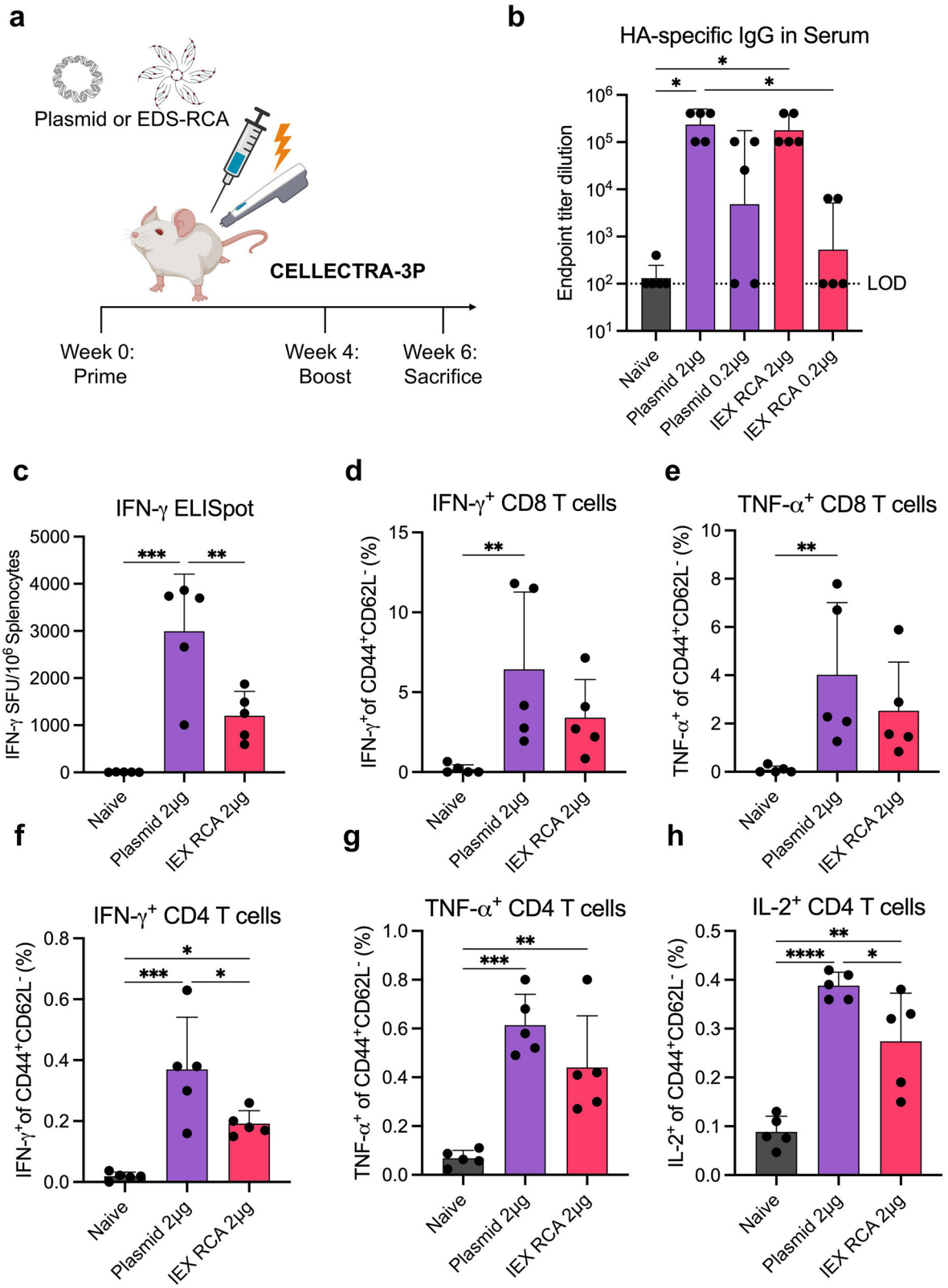

immune cells, including professional antigen-presenting cells. Our findings are consistent with published studies comparing the immunogenicity of plasmid DNA vaccines by GG versus electroporation[24–26]. Interestingly, EDS-RCA DNA and plasmid vaccines induced more comparable immune responses when administered via an adaptive electroporation device (CELLECTRA-3P) that, unlike a pulse-waveform device (BTX AgilePulse), does not require anesthesia during vaccine administration. Further work is warranted to dissect the comparative impacts of device electrical field and delivery routes (e.g., tissue resistance) on vaccine immunogenicity. Irrespective of the device or delivery route, the vaccine generated by EDS-RCA was capable of robust neutralizing antibody responses and HAI titers greater than 1/40, a threshold that is generally associated with protective responses

Fig. 6 | Immunogenicity of plasmid and EDS-RCA DNA vaccines delivered to muscle via CELLECTRA-3P. Balb/cJ mice ($N = 5$ per group) were immunized via IM-EP using the CELLECTRA-3P device with identical DNA from Fig. 5 (plasmid chassis or IEX-purified EDS-RCA DNA). **a** Schematic of experimental design. Mice received a prime and one booster immunization and immune responses were measured 2 weeks after booster (week 6). **b** CA09 HA-specific total IgG in serum measured by ELISA. **c** IFN-γ- secreting cell responses as measured by ELISpot. Cytokine-expressing effector $CD8^+$ or $CD4^+$ T cell populations as measured by flow cytometry: IFN-γ^+ $CD8^+$ T cells (**d**), TNF-α^+ $CD8^+$ T cells (**e**), IFN-γ^+ $CD4^+$ T cells (**f**), TNF-α^+ $CD4^+$ T cells (**g**), IL-2^+ $CD4^+$ T cells (**h**). Cells were pre-gated on live $CD3^+$ $CD8^+$ $CD4^-$ $CD44^+$ $CD62L^-$ **d**, **e** or live $CD3^+$ $CD8^-$ $CD4^+$ $CD44^+$ $CD62L^-$ (**f**–**h**). One way ANOVA (adjusted for multiple comparisons with Tukey's correction, **c**, **f**–**h**) or non-parametric Kruskal–Wallis ANOVA with multiple comparisons (**b**, **d**, **e** for data deemed non-normal by Shapiro–Wilk test) were used to compare groups. Error bars represent geometric mean with geometric standard deviation (**b**) or mean with standard deviation (**c**–**h**), dots represent individual mice, $^*p < 0.05$, $^{**}p < 0.01$, $^{***}p < 0.001$, $^{****}p < 0.0001$. Figures were generated using GraphPad Prism version 10.6 (GraphPad Software, Boston, MA, USA). Plasmid illustration is from NIAID NIH BioArt Source (bioart.niaid.nih.gov/bioart/411). Additional illustrations were created in BioRender. Tursi, N. (2026) https://BioRender.com/nj2lwa2.

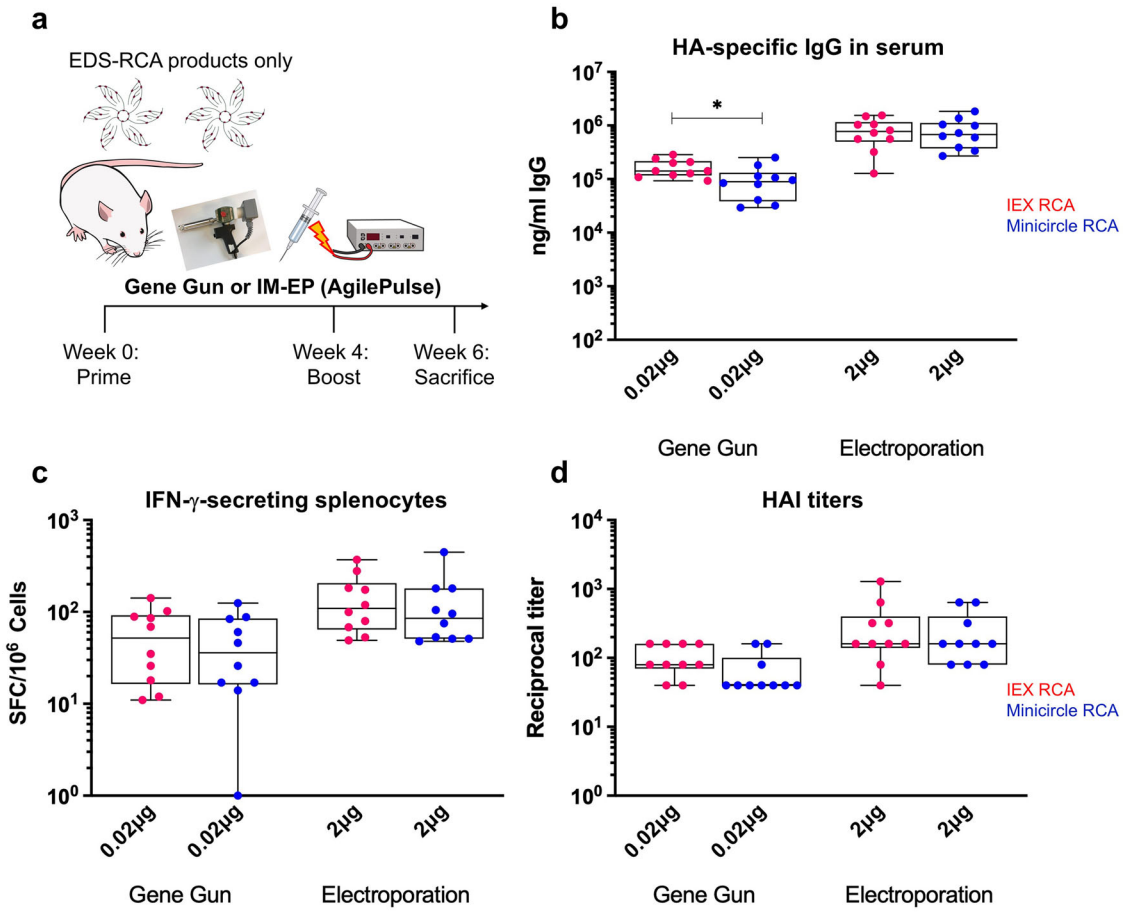

Fig. 7 | Immunogenicity of plasmid-templated EDS-RCA and minicircle-based EDS-RCA influenza HA DNA vaccines. Balb/c mice ($N = 10$ per group) were immunized via gene gun or electroporation, using the indicated optimum doses from Fig. 3. Minicircle-based EDS-RCA DNA vaccine (after three rounds of enzymatic error reduction and purification by ion exchange chromatography) was tested against plasmid-templated EDS-RCA DNA (using identical IEX RCA from Fig. 5). **a** Schematic of experimental design. Mice were primed and boosted 4 weeks apart and immune responses were measured 2 weeks after booster (week 6). **b** HA-specific antibody responses in serum measured by ELISA. **c** IFN-γ T cell responses measured by ELISpot. **d** Hemagglutinin inhibition (HAI) titers measured against virus. Whisker plots display min to max values for each group, dots represent individual mice. Mann–Whitney U test (two-tailed) was used for comparison between groups. $^*p < 0.05$. Figures were generated using GraphPad Prism version 10.4.2 for macOS (GraphPad Software, Boston, MA, USA). Certain illustrations are from NIAID NIH BioArt Source (bioart.niaid.nih.gov/bioart/283, bioart.niaid.nih.gov/bioart/506, bioart.niaid.nih.gov/bioart/580).

in vivo[38]. In addition, the EDS-RCA vaccine induced strong cellular responses on par with plasmid DNA vaccine. Taken together, we conclude EDS-RCA and plasmid vaccine chassis are functionally equivalent depending on the administration route and delivery device.

Recently, a DNA vaccine encoding neoantigens for hepatocellular carcinoma and delivered using CELLECTRA-3P has achieved potent immunogenicity in the clinic, including robust de novo neoantigen-specific $CD8^+$ T cell responses[39]. Notably, in the present study, we find that EDS-RCA DNA delivered using the same CELLECTRA device also induced significant $CD8^+$ T cell responses. Since robust $CD8^+$ T cell responses (in addition to $CD4^+$ T cells) are desired for cancer vaccines[40], it is possible the EDS-RCA method could provide a more rapid, cost-effective approach to develop and produce personalized cancer antigens. In this regard, EDS-RCA represents an important new methodology that warrants further study for neoantigen vaccine contexts.

Our EDS-RCA workflow addresses several shortcomings of conventional DNA production by bacterial fermentation. First, being completely synthetic, EDS-RCA can generate DNA in faster timelines than cell-based bioprocessing. We estimate that oligo printing, gene assembly, and RCA scale-up to gram-outputs of DNA can be achieved in as short as 3 days for subunit vaccines like HA (Supplemental Fig. S5). These time-savings are achieved by co-locating DNA printing and scale-up in the same location,

versus the current state-of-art of shipping oligos and dsDNA fragments by air and ground transportation (Supplementary Fig. S5). Second, by virtue of being completely synthetic, EDS-RCA simplifies downstream purification (and associated quality specifications). For example, no host cell protein or RNA contaminants are generated in EDS-RCA (unlike plasmid fermentation), which shifts the burden of endotoxin monitoring onto pre-qualified reagent inputs (versus laborious in-process removal of endotoxin during plasmid manufacturing). A key limitation of existing plasmid DNA vaccines (as currently delivered by electroporation or PharmaJet®) is that high DNA doses (1–5 mg) are required for sufficient immunogenicity in humans[39,41–43]. This increases both the cost per dose and the amount of time to produce sufficient doses for widespread vaccination campaigns. By eliminating requirements for cell-based manufacturing, synthetic EDS-RCA DNA vaccines could be manufactured at greater speed, purity, and scale than plasmid DNA, thereby enabling a more rapid response to emerging infectious diseases (at the population level) and accelerated personalized treatments for cancer and other chronic diseases (at the individual level).

Our current study is not without certain limitations. All in vivo studies were conducted in mice, so verifying these results in larger animals (such as swine) is a future goal. Portions of the EDS-RCA workflow presented herein were carried out manually, so increased workflow automation is a key goal, along with eliminating cold-chain maintenance of raw materials through reagent/enzyme lyophilization. Because it is unclear how many expression-competent copies of full-length double-stranded genes are generated by the RCA concatemer (versus single-stranded DNA and branched replication forks), a molar comparison to plasmid cannot be determined, so we have used DNA mass as a dose comparator. This means there is comparative uncertainty in how many expression-competent copies were actually delivered by EDS-RCA vaccines relative to plasmid DNA copies. Finally, while we have achieved DNA sequence fidelities that meet a threshold shared with mRNA vaccines, further work is needed to obtain EDS-RCA fidelities lower than ~0.01–0.02% average error per base to rival the best of what mRNA synthesis is expected to achieve.

Methods

Plasmid DNA preparation

Unless otherwise stated, enzymatically-synthesized HA (GenBank PV750927) was cloned into pCAGG-MCS-WPRE, which was constructed as follows: starting from pCAGG-MCS (PVT19755, Life Science Market), a custom gBlock fragment (IDT) corresponding to a strong WPRE enhancer[44] was cloned into the XhoI and BglII positions of the multiple cloning site, resulting in a CAGG promoter and WRPE combination that has been shown to enhance the efficacy of DNA vaccines[45]. Enzymatically-synthesized HA assemblies were subsequently cloned into the AflII and XhoI sites of pCAGG-MCS-WPRE. Purified pCAGG-HA-WPRE plasmids were prepared from *E. coli* clone pools or from a single clonally-isolated (Sanger-perfect) colony using endotoxin-free plasmid DNA purification kits (Qiagen #12362 and #12381). A minicircle vectorette version of pCAGG-MCS-WPRE was prepared by restriction digest to excise the ampicillin resistance gene and bacterial origin of replication, and enzymatically-synthesized HA (GenBank PX367232) was cloned into the vectorette. Mouse codon-optimized HA was chemically synthesized and cloned into a DNA vaccine plasmid essentially as described for pPML7800[46].

DNA preparation by EDS-RCA

The HA gene of the Swine California Flu virus (GenBank ACP41935.1) was computationally optimized for mammalian expression and DNA Script synthesis and assembly requirements, leveraging codon redundancy while removing any endogenous restriction sites (i.e., AflII, XhoI) that would compromise downstream cloning schemes. A mammalian-optimized Kozak sequence (5'-gccggcaccatg-3') was computationally inserted upstream of the HA coding sequence and flanking restriction sites (e.g., AflII, XhoI) were placed at the immediate 5' and 3' ends for downstream cloning. This in silico sequence was transferred to the console software of the SYNTAX® system, which proceeds automatically with the design and printing of the oligos and supports every step of the subsequent gene assembly.

All oligonucleotides used for EDS-RCA were printed on the SYNTAX System (DNA Script). The SYNTAX platform (consisting of the SYNTAX System, kits, and software) enables automated nucleic acid synthesis using TdT enzyme and subsequently desalts, quantifies, and normalizes the printed oligos across a 96-well plate. Oligo synthesis proceeds on an initiator DNA anchored to a solid support. At each cycle of synthesis, the TdT enzyme extends the initiator DNA by one nucleotide and further addition of residues is prevented by a reversible terminator group. Upon deprotection, the growing oligonucleotide chain is available for a new cycle. Once the desired oligonucleotide sequence has been completed, the oligonucleotide is enzymatically cleaved from its solid support and subsequently desalted, quantified, and normalized. Oligos for the HA gene were generated using commercially available SYNTAX 96 Hi-Fidelity kits (DNA Script) and synthesized oligos were verified by capillary electrophoresis using an Oligo Pro II (Agilent Biotechnologies).

Gene assembly was performed in two successive steps, starting with assembly of complementary oligonucleotides into short double stranded DNA blocks using a ligation-based method (referred to as "Step 1" Ligation in Fig. 1, middle panel) and ending with assembly of these short dsDNA blocks into a full-length HA gene using PCR (referred as "Step 2" PCR in Fig. 1). Block and gene sizes were confirmed by capillary electrophoresis using a Fragment Analyzer (Agilent Biotechnologies). Where indicated, a proprietary error-reduction process was introduced between Step 1 Ligation and Step 2 PCR to improve block and gene sequence fidelity. DNA quantification was performed by fluorescent DNA measurement on a Qubit-flex with Qubit DNA High Sensitivity Kit (Thermo Fisher Scientific).

HA gene assemblies and pCAGG-MCS-WPRE backbone were digested with AflII and XhoI enzymes and ligated with T4 DNA ligase (NEB), and corresponding ligation products were transformed into One Shot TOP10 competent cells (Thermo Fisher Scientific). An average of 300 colonies were picked and confirmed by PCR for the insert-backbone ligation junction. Approximately 200–250 individual clones were pooled to reconstitute a stock that is representative of the starting diversity of EDS HA assemblies. Plasmid DNA extracted from this bacterial pool was then used for rolling circle amplification. Plasmid DNA extracted from a single colony confirmed by Sanger sequencing (perfectly matching the reference HA sequence) is hereby referred to as "Sanger-perfect clone" and subsequently used as a reference and benchmark. Where indicated, HA gene assemblies were also cloned directly into a minicircle vectorette version of pCAGG-MCS-WPRE (i.e., devoid of ampicillin resistance gene and bacterial origin of replication) and ligated products were digested with exonuclease to remove non-circular DNA prior to rolling circle amplification.

RCA reactions were performed at milliliter scales (2 –20 ml) to generate milligram quantities of RCA DNA (range 1–13 mg). RCA reactions contained phi29 DNA polymerase, nucleotides, and modified random hexamers sourced from Cytiva. The generated RCA DNA product was subsequently purified by ethanol-based precipitation or ion exchange chromatography using proprietary methods. RCA DNA was formulated into TE or physiological saline for mouse immunization.

DNA sequencing

Oligonucleotides were sequenced using the ACCEL-NGS® 1S Plus DNA Library Kit (IDT). DNA blocks were prepared for sequencing using NEBNext Ultra II DNA Library Prep Kit for Illumina (NEB) along with dual index (NEBNext Multiplex Oligos for Illumina; NEB). Oligonucleotides were sequenced on an iSeq sequencer with iSeq Reagent Kit v2 (Illumina) while DNA blocks were sequenced on the MiSeq sequencer with MiSeq Reagent Kit v3 (Illumina). Full-length HA assemblies and PCR-amplicons derived from plasmid- or minicircle- clones were prepared for sequencing using the SMRTbell Barcoded Adapter Complete Prep Kit-96 and the SMRTbell DNA Damage Repair Kit (Pacific Bioscience). Long read sequencing was performed on the Sequel II sequencer with SMRTcells 8 M wells flowcell (Pacific Bioscience). Care was taken to avoid error

introduction during the PCR step preceding SMRTbell addition, as the choice of DNA polymerase was found to play a role in the reported error rate of the Sanger-perfect plasmid (see Supplementary Fig. S2).

PacBio long read data were processed using the default basecalling and filtering parameters for circular consensus sequencing (CCS) reads on the instrument to generate unaligned BAM files. During this step, each CCS read is tagged with the predicted accuracy, or read quality (rq), which is the average per-base log-likelihood ratio between the most likely template sequence and all alternative counterparts[47]. Unaligned BAM files were thresholded into four different read qualities (0.99, 0.999, 0.9999, 1), where 0.99 is the default threshold for PacBio CCS reads[47], and converted to fastqs using samtools fastq (v1.20)[48]. Reads were then aligned to their respective reference (GenBank PV750927 or PX367232) with minimap2 --secondary=no -ax map-hifi (v2.28)[49] and filtered with samtools view -F 2308 (v1.20)[48]. For digested RCA products, the gene and vector fragments were treated as separate references and only reads that unambiguously mapped to the gene fragment were used for read count and error rate calculations. The percent of mapped reads passing each filter was determined using the number of mapped reads with total reads of rq ≥0.99 as the denominator. Variants (insertions, deletions, mismatches) in the gene insert for both the PCR amplicons and RCA digests were quantified and parsed using bam-readcount (v1.0.1)[50] with minimum mapping quality set to 30. The rate of deletions, insertions, and mismatches at each position in the gene insert were then averaged and multiplied by 100. PacBio long reads were subsequently translated in silico to decipher the percentage of full-length protein supported by the gene assembly.

DNA delivery into epidermis using gene gun

Animal studies were conducted under protocols approved by the University of Washington Institutional Animal Care and Use Committee (IACUC). Six-to-eight-week-old female BALB/cHsD (Envigo RMS, Indianapolis, IN) were used in these studies. Animals were acclimated to the vivarium for between 3 and 7 days prior to vaccination.

Plasmid or RCA DNA were coated onto gold particles as follows: 25 mg of 57-0 gold particles (Technic, Inc) were suspended in 150 µl 50 mM spermidine (Sigma, S0266), followed by the addition of 50 µl of DNA (at the prescribed dose), and 150 µl of 10% calcium chloride (McKesson, 1091140) while vortexing. The mixture was then incubated statically for ten minutes at room temperature (RT). The DNA-coated gold particles were then washed by pulling off the supernatant, resuspending the particles in absolute ethanol, and vortexing for 10 s for each wash. After the final wash, the DNA-coated beads were resuspended in 3.2 ml ethanol and briefly vortexed immediately before loading into a 25" piece of ETFE tubing (McMaster-Carr, 5583K44) that was inserted into an automated "Tube Turner" (legacy PowderJect Vaccines equipment) that is now marketed by Bio-Rad (Tubing Prep Station, 1652418). The tube turner automatically distributes the DNA coated gold particles evenly across the inside of the ETFE tubing (3/32" inner diameter) and removes the ethanol. After drying for two hours under a stream of nitrogen the tubing was cut into half-inch piece cartridges. One dose consists of two cartridges that are administered into two adjacent sites on the skin. When combined, these deliver one milligram of gold coated with the prescribed dose amount of DNA used for this study (20 ng – 2 µg).

Mice were anesthetized with a ketamine/xylazine drug mixture, bled to collect pre-immune sera, and abdominal fur was clipped. Using the XR1 gene delivery device (legacy PowderJect Vaccines equipment, formerly known as Accell® GG)[51], each animal was immunized with the indicated DNA doses and returned to housing. At four weeks post-prime, the animals were again anesthetized, bled, and boosted with the same dose. At two weeks post-boost, the animals were euthanized and blood, spleens, and lungs were collected for analysis. All animals on study are reported and were not blinded during the study. The study duration (i.e., 6 weeks, comprising prime and boost vaccine delivery) facilitated comparisons of peak immunogenicity.

BTX AgilePulse intramuscular delivery of DNA

Animal studies were conducted under protocols approved by the University of Washington Institutional Animal Care and Use Committee (IACUC). Six-to-eight-week-old female BALB/cHsD (Envigo RMS, Indianapolis, IN) were used in these studies. Animals were acclimated to the vivarium for between 3 and 7 days prior to vaccination. Mice were anesthetized with a ketamine/xylazine drug mixture, bled to collect pre-immune sera, and the area over both tibialis anterior muscles was shaved with a surgical prep clipper. Using the AgilePulse ID Electroporation System delivery device (BTX, Holliston, MA), each mouse was immunized bilaterally in each tibialis anterior muscle with the indicated doses of DNA vaccine (diluted in saline) evenly between the two muscles and returned to housing. The electroporation cycles (which were developed for plasmid DNA delivery) were as follows:

G1: 1 × 450 V, 50 µS duration, 200 µS pause; then G2: 1 × 450 V, 50 µS duration, 50 mS pause; then G3: 8 × 110 V, 10 mS, 20 mS pause between repeats.

At four weeks post-prime, the mice were again anesthetized, bled, and boosted with the same dose. At 2 weeks post-boost, the mice were euthanized, and blood, spleens, and lungs were collected for analysis. All animals on study are reported and were not blinded during the study. The study duration (i.e., 6 weeks, comprising prime and boost vaccine delivery) facilitated comparisons of peak immunogenicity.

CELLECTRA-3P intramuscular delivery of DNA

Animal studies involving adaptive electroporation were conducted under protocols approved by the Wistar Institute Institutional Animal Care and Use Committee (IACUC). Six-to-eight-week-old female BALB/cJ (Jackson Laboratory) were housed in the Wistar Institute Animal Facility. Animals were randomized by the Animal Facility upon arrival. Mice were immunized twice with the indicated plasmid DNA or EDS-RCA constructs at 2 or 0.2 µg (formulated in water) into the tibialis anterior muscle followed by in vivo adaptive electroporation using the CELLECTRA-3P device (Inovio Pharmaceuticals) and manufacturer-recommended protocols for plasmid DNA delivery. Mice were bled by submandibular bleed for assessment of serum antibody responses. At 6 weeks post-immunization, mice were euthanized using CO_2 and blood and spleens were harvested for analysis. All animals on study are reported and were not blinded during the study. The study duration (i.e., 6 weeks, comprising prime and boost vaccine delivery) facilitated comparisons of peak immunogenicity (Supplementary Fig. S4).

ELISA

Following standard procedures at University of Washington, an indirect ELISA procedure was used to measure antibody levels in serum isolated in MiniCollect tubes (Greiner Bio-One, 450472). Briefly, Costar 3590 ELISA plates were coated with either 50 ng/well recombinant California/04/2009 HA (Sino Biologicals, 11055-V08B) or dilutions of mouse IgG (Sigma, I5381) to establish a standard curve. Serum samples were serially diluted and plated in HA containing wells (the highest dilution from post-boost animals was 1/48,600). Goat anti-mouse IgG/ HRP (Southern Biotech, 1033-05) was used to detect HA bound IgG. Sure-Blue HRP substrate (Seracare, 5120-0077) was added and incubated for fifteen minutes and stopped by the addition of 2 N sulfuric acid. The plate was immediately read on an Emax plate reader (Molecular Diagnostics, Inc.) and Emax software was used to calculate antibody concentrations.

Following standard procedures at the Wistar Institute, an indirect ELISA procedure was used to measure antibody levels in serum using high-binding 96-well half-area plates (Corning, 3690) that were coated with 1 µg/ml of H1N1 A/California/04/2009 HA protein (Sino Biologicals, 11055-V08H) in PBS overnight at 4°C. The next day, plates were washed 4 times with PBS containing 0.05% Tween-20 (PBS-T) before blocking with 1× PBS containing 5% dry milk (LabScientific) and 0.2% Tween-20 (Fisher) for 1 h at RT. The plates were washed and incubated with serially diluted mouse serum in 1% newborn calf serum and 0.2% Tween-20 in 1x DPBS (ELISA diluent) for 2 h at RT. The plates were then washed and incubated with HRP-conjugated Goat anti-mouse IgG H + L (Bethyl, A90-216P) for 1 h at

RT in ELISA diluent, and then washed and developed with 1-Step™ TMB Ultra (Thermo Fisher Scientific, 34029) for 5 miN at RT before being stopped with 2 N H_2SO_4. The plates were read on a BioTEK Synergy 2 plate reader at 450 and 570 nm absorbance values. OD values were background corrected by subtracting 570 nm values from 450 nm values. Endpoint titers were calculated against naïve mouse serum and defined as the highest dilution where the OD value was greater than cutoff determined using the following formula: Average (Naïve Mice) + (4 × SD (Naïve Mice)).

Hemagglutination inhibition assay

The following reagent was obtained through BEI Resources, NIAID, NIH: Influenza A Virus, A/California/07/2009 (HA, NA) × A/Puerto Rico/8/1934 (H1N1) pdm09, Reassortant NYMC X-181, NR-44004

The protocol was conducted as defined by the "WHO Manual on Animal Influenza Diagnosis and Surveillance" publication WHO/CDS/CSR/NCS/2002.5. Briefly, 150 µl of Receptor Destroying Enzyme (RDE, Hardy Diagnostics 370013) was added to 50 µl of sera and incubated overnight at 37 °C. The RDE was inactivated by heating samples to 56 °C for 45 min and samples diluted by addition of 300 µl PBS. Samples were then serially diluted in 96-well V-bottom plates (Corning, 3898) and titered virus stock (BEI NR-44004 or mouse-adapted Ca04/09, which is a kind gift from Richard J. Webby, Department of Infectious Diseases, St. Jude Children's Research Hospital, Memphis, Tennessee 38105-3678) was added to each well. After 15 min, 0.5% washed turkey red blood cells (HemoStat Laboratories TBA030) were added and allowed to sit for 30 min. Plates were then tilted and read to determine highest dilution that inhibited hemagglutination.

Virus neutralization assay

The following reagent was obtained through BEI Resources, NIAID, NIH: Influenza A Virus, A/California/04/2009 (H1N1) pdm09, Cell Isolate (Produced in Cells), NR-13658.

Serum samples were prepared with Receptor Destroying Enzyme (RDE, Hardy Diagnostics 370013) identically to the hemagglutination inhibition assay. Samples were serially diluted with PBS in 96-well V-bottom plates (Corning 3898) leaving 60 µl in each well, to which 60 µl of 100 TCID50 / 50 µl virus (BEI NR-13658) was added and incubated 15 min at RT. One hundred microliters from each well were transferred to confluent MDCK cells washed with virus growth media (DMEM/ 0.3% BSA/ 25 mM HEPES/ 1 µg/ml TPCK-Trypsin) and incubated for two hours in a 37 °C CO_2 incubator. This mixture was removed, the plates were washed once with virus growth media, then 200 µl of fresh virus growth media was added to each well and the plates were incubated for three days at 37 °C in CO_2 incubator. On day three, 50 µl of cell supernatant was added to 50 µl of 0.5% washed turkey red blood cells and allowed to sit for 30 min. The plates were then tilted and read to determine the highest dilution that neutralized the virus.

Preparation of single cell lung and spleen suspensions

At the University of Washington, lungs were minced with scissors, transferred to 10 ml digestion buffer (750 µg/ml DNase (Sigma, DN25) and 1.2 mg/ml collagenase (Life Technologies, 17101015) in RMPI (Thermo Fisher Scientific, 11875-030) and incubated for 45 min at 37 °C; cells were then strained through a 70-micron strainer (Fisher, 170-3554) and collected by centrifugation. Spleens were also pressed through a 70-µm strainer to release splenocytes and cells were collected by centrifugation. After centrifugation, cell pellets were treated with ACK lysis buffer (Thermo Fisher Scientific, A10492-01) to lyse red blood cells. Splenocytes and lung cells were then washed twice with RPMI/5% FCS (VWR, 89510-188) and cell concentrations were determined using a T4 Cell Counter (Nexcellom) and adjusted to 5×10^6 cells/ml in stimulation media "SM" (RPMI/10% FCS supplemented with sodium pyruvate, Thermo Fisher Scientific, 11360-070) and non-essential amino acids (Thermo Fisher Scientific, 11140-050).

At the Wistar institute, spleens were harvested into ice cold RPMI 1640 + 10% fetal bovine serum (FBS) + 1% penicillin/streptomycin (R10) and mechanically dissociated using a Stomacher 80 (Seward). The isolated splenocytes were then filtered using a 40 µm strainer before Ammonium-Chloride-Potassium (ACK) lysis for 5 min at RT. The cells were quenched by dilution with PBS and resuspended in fresh R10 before a second 40 µm filtration. The splenocytes were then counted using a ViCell Blu Cell Viability Analyzer (Beckman Coulter) and subjected to downstream assays.

IFN-γ ELISPOT

The following peptide reagents were obtained through BEI Resources: Influenza Virus A/California/07/2009 (H1N1) pdm09 Hemagglutinin Protein, NR-19244.

At the University of Washington, 96-well plates (Millipore, MAIPS4510) were pre-wetted and washed according to the manufacturer's instructions. Each well was coated with 500 ng rat anti-mouse IFN-γ (Becton Dickinson, BDB551216) in PBS and incubated overnight at 4 °C. Prior to tissue harvesting the next morning, plates were washed with PBS and blocked with SM stimulation media. Prior to plating the cells, SM was removed from the wells. Rows A and B (negative controls) were loaded with 50 µl of SM, rows C-F (test wells) were loaded with 50 µl HA peptides (BEI NR19244 pool of peptides # 8, 9, 10, 30, 31, 32, 115, 116, 132, 133, 134 at a final concentration of 2 µg/ml for each peptide), and rows G and H (positive controls) were loaded with 50 µl concanavalin A (Sigma, C2272) at final concentration of 10 µg/ml). Approximately 2.5×10^5 cells (50 µl) isolated from spleen and lung cell samples were added to wells in an assigned column and incubated overnight (18–20 h) in humidified 37 °C/ 5% CO_2 incubator. The plates were then washed and incubated for two hours with 50 µl of a 1 µg/ml solution of biotin-conjugated rat anti-mouse IFN-γ (Becton Dickinson, BDB554410) in PBS, washed, and incubated for one hour with 50 µl of 1 µg/ml streptavidin/alkaline phosphatase conjugate (BioRad, 170-3554) in PBS. After washing, the spots were developed with 50 µl AP Conjugate Substrate kit (BioRad, 170-6432) for 13–15 min, washed, dried, and counted on ELISPOT plate reader (Cellular Technologies, LTD).

At the Wistar Institute, mouse IFN-γ ELISpot plates (Mabtech) were used according to the manufacturer's protocol. Briefly, the plates were washed in sterile PBS four times before blocking in complete R10 for 30 min at RT. The plates were then seeded with 1×10^5 cells in duplicate in the presence of 5 µg/ml of overlapping CA09 HA peptide pools (15 amino acids with 9 amino acid overlap). DMSO or Cell Stimulation Cocktail (eBioscience) were used as negative and positive controls, respectively. The plates were incubated for 20 hours at 37 °C in 5% CO_2 before being developed according to the manufacturer's protocol. The spots were counted using a Mabtech IRIS (Mabtech). Counts after peptide stimulation were reported after subtracting values from negative controls.

Flow cytometry

Splenocytes were plated and incubated in the presence of Protein Transport Inhibitor Cocktail (eBioscience) and overlapping CA09 HA peptides. Negative control samples were stimulated in the presence of dimethyl sulfoxide (DMSO) and positive control samples in the presence of Cell Stimulation Cocktail (eBioscience). Splenocytes were first stimulated for 6 h at 37 °C and then washed in PBS before incubation with Zombie Aqua viability dye (Biolegend) for 10 min at RT. Cells were washed in 0.2% BSA in PBS (FACS buffer) and resuspended in cocktail of antibodies targeting surface molecules for 30 min at ambient temperature containing: BUV395 anti-mouse CD3e (Clone 17A2, BD), BUV805 anti-mouse CD62L (Clone MEL-14, BD), BV421 anti-mouse CD4 (Clone GK1.5, Biolegend), BV605 anti-mouse CD44 (Clone IM7, Biolegend), and APC-Cy7 anti-mouse CD8a (Clone 53-6.7, Biolegend). The cells were then washed in FACS before fixation/permeabilization using BD CytoFast/CytoFix (BD) according to manufacturer's protocol for 20 min at 4°C. Fixed cells were washed in 1× Perm/Wash (from kit) before being stained with the following intracellular stain cocktail for 30 λ min at 4 °C: PE anti-mouse TNF-α (Clone MP6-XT22, Biolegend), PE-Cy7 anti-mouse IL-2 (Clone JES6-5H4, Biolegend), and APC anti-mouse IFN-γ (Clone XMG1.2, Biolegend). The cells were resuspended in FluoroFix buffer (Biolegend) and stored at 4 °C until

acquisition using a BD FACSymphony A3. Cytokine/marker expressing $CD4^+$ and $CD8^+$ T cell populations were defined as cytokine/marker+ and are shown as a percent of $CD44^+$ $CD62L^-$ effector cells.

Statistical analysis

GraphPad Prism 10 and Excel (Microsoft 365) were used for graphs and statistical analysis. Normality was tested with either Shapiro–Wilk or the D'Agostino and Pearson tests. Mann-Whitney U test (two-tailed) was used for comparison between two groups. For data deemed normal, a one-way ANOVA with Tukey's multiple comparisons correction was performed. For data deemed non-normal, a Kruskal–Wallis ANOVA adjusted or Dunn's multiple comparison was used for comparison between three or more groups. P-values < 0.05 are considered statistically significant, while p-values > 0.05 are not reported. Where indicated in the legends, graphs show either min to max values per group, mean with standard deviation, or geometric mean and standard deviation.

Data availability

The DNA sequence encoding HA and in silico optimized for enzymatic DNA synthesis was deposited to GenBank (accession number PV750927). An enzymatically-optimized HA variant (GenBank PX367232, containing R238K residue for production batch-tracking purposes) was also deposited. PacBio sequencing data generated by this study can be retrieved from the Sequence Read Archive (SRA) under the BioProject ID PRJNA1329312.

Code availability

Computational code used for sequence analysis is hosted on GitHub (see https://github.com/timplab/pacbio_eds_rca).

Received: 12 June 2025; Accepted: 22 November 2025;
Published online: 13 December 2025

References

1. Ashley, J., Potts, I. M. & Olorunniji, F. J. Applications of terminal deoxynucleotidyl transferase enzyme in biotechnology. *ChemBioChem* **24**, e202200510 (2023).
2. Challener, C. A. Synthetic DNA as an alternative to plasmids. *BioPharm. Int.* **37**, 14–17 (2024).
3. Ohlson, J. Plasmid manufacture is the bottleneck of the genetic medicine revolution. *Drug Discov. Today* **25**, 1891–1893 (2020).
4. Conforti, A. et al. Linear DNA amplicons as a novel cancer vaccine strategy. *J. Exp. Clin. Cancer Res.* **41**, 195 (2022).
5. Vilalta, A. et al. Vaccination with polymerase chain reaction-generated linear expression cassettes protects mice against lethal influenza A challenge. *Hum. Gene Ther.* **18**, 763–771 (2007).
6. Shen, X. et al. Influenza A vaccines using linear expression cassettes delivered via electroporation afford full protection against challenge in a mouse model. *Vaccine* **30**, 6946–6954 (2012).
7. Moreno, S. et al. DNA immunisation with minimalistic expression constructs. *Vaccine* **22**, 1709–1716 (2004).
8. Hughes, R. A. & Ellington, A. D. Synthetic DNA synthesis and assembly: putting the synthetic in synthetic biology. *Cold Spring Harb. Perspect. Biol.* **9** https://doi.org/10.1101/cshperspect.a023812 (2017).
9. de Mey, W. et al. A synthetic DNA template for fast manufacturing of versatile single epitope mRNA. *Mol. Ther. Nucleic Acids* **29**, 943–954 (2022).
10. Hekele, A. et al. Rapidly produced SAM® vaccine against H7N9 influenza is immunogenic in mice. *Emerg. Microbes Infect.* **2**, 1–7 (2013).
11. Dormitzer, P. R. et al. Synthetic generation of influenza vaccine viruses for rapid response to pandemics. *Sci. Transl. Med.* **5**, 185ra168–185ra168 (2013).
12. Simmons, B. L., McDonald, N. D. & Robinett, N. G. Assessment of enzymatically synthesized DNA for gene assembly. *Front. Bioeng. Biotechnol.* **11** https://doi.org/10.3389/fbioe.2023.1208784 (2023).
13. Hutchison, C. A., Smith, H. O., Pfannkoch, C. & Venter, J. C. Cell-free cloning using φ29 DNA polymerase. *Proc. Natl. Acad. Sci. USA* **102**, 17332–17336 (2005).
14. Dean, F. B., Nelson, J. R., Giesler, T. L. & Lasken, R. S. Rapid amplification of plasmid and phage DNA using Phi 29 DNA polymerase and multiply-primed rolling circle amplification. *Genome Res.* **11**, 1095–1099 (2001).
15. Kendirgi, F. et al. Novel linear DNA vaccines induce protective immune responses against lethal infection with influenza virus type A/H5N1. *Hum. Vaccines* **4**, 410–419 (2008).
16. de Graaf, J. F. et al. Neoantigen-specific T cell help outperforms non-specific help in multi-antigen DNA vaccination against cancer. *Mol. Ther. Oncol.* **32**, 200835 (2024).
17. Scott, V. L. et al. Novel synthetic plasmid and Doggybone DNA vaccines induce neutralizing antibodies and provide protection from lethal influenza challenge in mice. *Hum. Vaccine Immunother.* **11**, 1972–1982 (2015).
18. Walters, A. A. et al. Comparative analysis of enzymatically produced novel linear DNA constructs with plasmids for use as DNA vaccines. *Gene Ther.* **21**, 645–652 (2014).
19. Masaki, Y., Onishi, Y. & Seio, K. Quantification of synthetic errors during chemical synthesis of DNA and its suppression by non-canonical nucleosides. *Sci. Rep.* **12**, 12095 (2022).
20. Filges, S., Mouhanna, P. & Ståhlberg, A. Digital quantification of chemical oligonucleotide synthesis errors. *Clin. Chem.* **67**, 1384–1394 (2021).
21. Ma, S., Saaem, I. & Tian, J. Error correction in gene synthesis technology. *Trends Biotechnol.* **30**, 147–154 (2012).
22. Potapov, V. et al. A single-molecule sequencing assay for the comprehensive profiling of T4 DNA ligase fidelity and bias during DNA end-joining. *Nucleic Acids Res.* **46**, e79 (2018).
23. Potapov, V. et al. Comprehensive profiling of four base overhang ligation fidelity by T4 DNA ligase and application to DNA assembly. *ACS Synth. Biol.* **7**, 2665–2674 (2018).
24. Pertmer, T. M. et al. Gene gun-based nucleic acid immunization: elicitation of humoral and cytotoxic T lymphocyte responses following epidermal delivery of nanogram quantities of DNA. *Vaccine* **13**, 1427–1430 (1995).
25. Wang, S. et al. The relative immunogenicity of DNA vaccines delivered by the intramuscular needle injection, electroporation and gene gun methods. *Vaccine* **26**, 2100–2110 (2008).
26. Fynan, E. F. et al. DNA vaccines: protective immunizations by parenteral, mucosal, and gene-gun inoculations. *Proc. Natl. Acad. Sci. USA* **90**, 11478–11482 (1993).
27. Nelson, J. R. et al. TempliPhi, phi29 DNA polymerase based rolling circle amplification of templates for DNA sequencing. *Biotechniques* **32**, 44–47 (2002).
28. Bradley, C. C. et al. RNA polymerase inaccuracy underlies SARS-CoV-2 variants and vaccine heterogeneity. *Res. Sq.* https://doi.org/10.21203/rs.3.rs-1690086/v1 (2022).
29. Chen, T. H., Potapov, V., Dai, N., Ong, J. L. & Roy, B. N(1)-methyl-pseudouridine is incorporated with higher fidelity than pseudouridine in synthetic RNAs. *Sci. Rep.* **12**, 13017 (2022).
30. Wong, H. E., Huang, C. J. & Zhang, Z. Amino acid misincorporation in recombinant proteins. *Biotechnol. Adv.* **36**, 168–181 (2018).
31. Harris, R. P. & Kilby, P. M. Amino acid misincorporation in recombinant biopharmaceutical products. *Curr. Opin. Biotechnol.* **30**, 45–50 (2014).
32. Amante, D. H. et al. Skin transfection patterns and expression kinetics of electroporation-enhanced plasmid delivery using the CELLECTRA-3P, a portable next-generation dermal electroporation device. *Hum. Gene Ther. Methods* **26**, 134–146 (2015).
33. Morrow, M. P. et al. DNA immunotherapy for recurrent respiratory papillomatosis (RRP): phase 1/2 study assessing efficacy, safety, and immunogenicity of INO-3107. *Nat. Commun.* **16**, 1518 (2025).

34. Marano, J. M., Chuong, C. & Weger-Lucarelli, J. Rolling circle amplification: a high fidelity and efficient alternative to plasmid preparation for the rescue of infectious clones. *Virology* **551**, 58–63 (2020).
35. Mizuta, R., Mizuta, M. & Kitamura, D. Atomic force microscopy analysis of rolling circle amplification of plasmid DNA. *Arch. Histol. Cytol.* **66**, 175–181 (2003).
36. Sato, M., Ohtsuka, M. & Ohmi, Y. Repeated GenomiPhi, phi29 DNA polymerase-based rolling circle amplification, is useful for generation of large amounts of plasmid DNA. *Nucleic Acids Symp. Ser.* **48**, 147–148 (2004).
37. Loghin, E. et al. Transient Transfection of Rolling-Circle Amplified DNA in Biomanufacturing-Relevant Mammalian Cell Lines: A Comparison of Transfection Conditions for Optimal Protein Expression. *Biotechnol. Appl. Biochem.* https://doi.org/10.1002/bab.70100 (2025).
38. Cox, R. J. Correlates of protection to influenza virus, where do we go from here? *Hum. Vaccine Immunother.* **9**, 405–408 (2013).
39. Yarchoan, M. et al. Personalized neoantigen vaccine and pembrolizumab in advanced hepatocellular carcinoma: a phase 1/2 trial. *Nat. Med.* **30**, 1044–1053 (2024).
40. Duperret, E. K. et al. A synthetic DNA, multi-neoantigen vaccine drives predominately MHC Class I CD8(+) T-cell responses, impacting tumor challenge. *Cancer Immunol. Res.* **7**, 174–182 (2019).
41. Khobragade, A. et al. Efficacy, safety, and immunogenicity of the DNA SARS-CoV-2 vaccine (ZyCoV-D): the interim efficacy results of a phase 3, randomised, double-blind, placebo-controlled study in India. *Lancet* **399**, 1313–1321 (2022).
42. Tebas, P. et al. Safety and immunogenicity of INO-4800 DNA vaccine against SARS-CoV-2: a preliminary report of an open-label, phase 1 clinical trial. *EClinicalMedicine* **31**, 100689 (2021).
43. De Rosa, S. C. et al. Robust antibody and cellular responses induced by DNA-only vaccination for HIV. *JCI Insight* **5** https://doi.org/10.1172/jci.insight.137079 (2020).
44. Zanta-Boussif, M. A. et al. Validation of a mutated PRE sequence allowing high and sustained transgene expression while abrogating WHV-X protein synthesis: application to the gene therapy of WAS. *Gene Ther.* **16**, 605–619 (2009).
45. Garg, S., Oran, A. E., Hon, H. & Jacob, J. The hybrid cytomegalovirus enhancer/chicken beta-actin promoter along with woodchuck hepatitis virus posttranscriptional regulatory element enhances the protective efficacy of DNA vaccines. *J. Immunol.* **173**, 550–558 (2004).
46. Loudon, P. T. et al. GM-CSF increases mucosal and systemic immunogenicity of an H1N1 influenza DNA vaccine administered into the epidermis of non-human primates. *PLoS ONE* **5**, e11021 (2010).
47. How does CCS work. *CCS Docs*. https://ccs.how/how-does-ccs-work.
48. Li, H. et al. The sequence alignment/map format and SAMtools. *Bioinformatics* **25**, 2078–2079 (2009).
49. Li, H. Minimap2: pairwise alignment for nucleotide sequences. *Bioinformatics* **34**, 3094–3100 (2018).
50. Ajay Khanna, D. E. L. et al. Bam-readcount - rapid generation of basepair-resolution sequence metrics. *J. Open Source Softw.* **7**, 3722 (2022).
51. Chen, D., Maa, Y. F. & Haynes, J. R. Needle-free epidermal powder immunization. *Expert Rev. Vaccines* **1**, 265–276 (2002).

Acknowledgements

We thank Nick Riddiford for assistance with sequence bioinformatics, and Sylvian Dubourg and Florence Mahé for assistance with DNA synthesis and assembly. We also thank Tyler Hammond, Craig Galligan, Lisa Lowery, Wei Gao, Alex Corwin, and Zhen Liu for assistance with reagent prep, DNA scale-up, and downstream purification. This work was funded by the Defense Advanced Research Project Agency (DARPA) under contract #N66001-21-C-4014 (awarded to GE). Portions of this work were also supported by DARPA and the Joint Program Executive Office for Chemical, Biological, Radiological and Nuclear Defense (JPEO-CBRN) (Award HR0011-21-9-0001). D.B.W. is additionally supported by NIH/NIAID Collaborative Influenza Vaccine Innovation Centers (CIVIC) contract 75N93019C00051, the W.W. Smith Charitable Trust Distinguished Professorship in Cancer Research, and the Jill and Mark Fishman Foundation. N.J.T. is supported by T32CA009171. The opinions, findings, and conclusion or recommendations expressed in this study are those of the authors and do not necessarily reflect the view of DARPA or the US government.

Author contributions

S.C. and R.R. lead enzymatic oligo synthesis and gene assembly. E.K., J.N., and W.G. lead DNA propagation, including rolling circle amplification and DNA purification. C.H. and W.T. conducted sequence analysis of the generated DNA. J.F., N.J.T., and K.B. performed DNA immunization and analyzed mouse results. X.G., D.B.W., J.N., W.G., E.K., and D.H.F. assisted in supervision and manuscript editing. E.K., N.J.T., S.C., and C.H. prepared the initial draft manuscript. All authors read and approved the final manuscript.

Competing interests

The authors declare the following, which may be considered as potential competing interests: S.C., R.R., and X.G. are employees of DNA Script and have filed patent applications pertaining to aspects of this work. E.K., J.N., and W.G. are employees of GE HealthCare and have filed patent applications pertaining to aspects of this work. D.B.W. is a consultant for and a member of the Scientific Advisory Board for INOVIO Pharmaceuticals. D.H.F. is a consultant for and co-founder of Orlance Inc. Neither Orlance nor INOVIO were involved in the study design, data collection, data analysis, or manuscript preparation. D.B.W. participates in industry collaborations; has received speaking honoraria; and has received fees for consulting, including serving on scientific review committees. Remunerations received by D.B.W. include direct payments and equity/options. D.B.W. also discloses the following associations with commercial partners: Geneos (consultant/advisory board), AstraZeneca (advisory board, speaker), and Pfizer (advisory board). All other authors declare that they have no competing interests related to this work.

Additional information

Supplementary information The online version contains supplementary material available at https://doi.org/10.1038/s41541-025-01329-0.

Correspondence and requests for materials should be addressed to Erik Kvam or Deborah H. Fuller.